

TEST: A Modular Scientific Nanosatellite

David L. Voss*, A. Kirchoff†, D. P. Hagerman‡, J.J. Zapf§, J. Hibbs¶, J. Dailey#, A. White**, H. D. Voss††
Taylor University, Upland, IN, 46989

and

M. Maple§§ and Farzad Kamalabadi ¶¶
University of Illinois, Urbana, IL, 61801

A powerfully instrumented, reliable, low-cost, and 3-axis stabilized nanosatellite is being developed as part of the Air Force University Nanosatellite-3 Program. The Thunderstorm Effects in Space: Technology (TEST) nanosatellite implements a new, highly modular satellite bus structure and common electrical interface that is conducive to satellite modeling, development, testing, and integration flow. TEST is a low-cost (\$0.2 M) nanosatellite (30kg) in final development by Taylor University and the University of Illinois. TEST implements a variety of plasma, energetic particle, and remote sensing instrumentation with the objective of understanding how lightning and thunderstorms influence the upper atmosphere and the near-space environment. The TEST modular design and instrumentation challenges portions of satellite systems (such as future DOD DMSP and NASA LWS Geospace Missions), while complementing large multi-probe and remote sensing programs. TEST includes a variety of proven instrumentation: two 1m Electric Field (EP) probes, a thermal plasma density Langmuir Probe (LP), a 5 to 100 kHz Very Low Frequency (VLF) Receiver, two large geometric factor cooled (-60° C) Solid State Detector (SSD) spectrometers for energetic electrons and ions ($10 \text{ keV} < E < 1 \text{ MeV}$), a 3-axis Magnetometer (MAG), a O₂ Hertzberg UV Photometer, a 391.4 nm Transient Photometer and a 630 nm Imager for airglow and lightning measurements. In addition, the satellite is three-axis stabilized using CO₂ band horizon sensors, as well as a two-stage passive radiator for instrument cooling. TEST instrumentation and satellite subsystems are packaged in modular cubes of 10 cm increments. A common modular electrical interface board is used to standardize each of the subsystems for data flow, ground support, and data analysis.

I. Introduction

The Thunderstorm Effects in Space Technology (TEST) nanosatellite is a student developed scientific satellite based on a highly modular design to reduce cost and increase design flexibility. By system level burn-in of industrial commercial-off-the-shelf (COTS) parts and quality-preferred parts, a cost-effective, and powerful nanosatellite has been rapidly prototyped and developed. The TEST satellite has direct application for science instrumentation where multi-data point measurements are desired, for remote sensing from a 3-axis stabilized bus, for new modular technologies, and for education.

* now graduate student at Boston University, Electrical Engineering, Dvoss@bu.edu, AIAA Student Member

† undergraduate Computer Engineering student, austin_kirchoff@taylor.edu

‡ undergraduate Computer Engineering student, dwayne_hagerman@taylor.edu, AIAA student Member

§ now graduate student at ECE Department, Purdue, Indianapolis,

¶ undergraduate Engineering Physics student, Jesse_Hibbs@tayloru.edu

Engineering Consultant

** Professor of Computer Science, arwhite@tayloru.edu

†† Professor of Physics, Hnvoss@taylor.edu, AIAA member

§§ Engineer now at Southwest Research Institute

¶¶ Assistant Professor of Electrical and Computer Engineering

II. Modularity

Electrical, mechanical, FEM modeling, and flight software modularity in a satellite design can significantly reduce cost and development time while maintaining system performance. However, drawbacks exist such as mechanical building block size increments and fixed attachment points. The TEST satellite has been designed with all subsystems filling 4” (or 10 cm) dimension cube modules, or a multiple of this base size.

The modular size increment is based on the CubeSat program¹ but is now taken one step further to pack the cubes into a three dimensional array (CubeSat^{cubed}). Modules are then plugged together in a 3-D pattern to form the shape of the overall satellite. The satellite is able to accommodate any box shape that is a multiple of 4” so that larger instruments and subsystems can be accommodated.

Breaking up subsystems into distinct modules has helped to define the satellite design early. The modular structure results in efficient and topologically complementary mechanical, electrical, and harness designs. By standardizing the size of modules, each subsystem is able to have a large degree of freedom in where it is placed with little impact on the other satellite subsystems as requirements mature. We found that we had to rearrange modules for unforeseen heat sinking requirements, optical bench requirements, pointing requirements, noise requirements, and science requirements. This modular placement freedom also results in innovative designs that allow for break-through technology to be implemented in various levels of the satellite development.

Although a modular satellite may help with design and construction, there are much greater benefits to modularity. Having a stock of qualified basic modules for distinctive communication links, attitude requirements, or power requirements would reduce satellite development turnaround time and integration time. Although modularity is a term that is used frequently in satellite papers and presentations, the space science industry has much to learn from its computer and automotive counterparts for developing a mass-produced constellation of reliable nanosatellites. A summary of modularity is given in Table 1.

Table 1. Nanosatellite Modularity Summary.

| | |
|---|---|
| A | Cubes can be rotated x,y,z due to standard structure & connectors |
| B | Mechanical advantages |
| | Early definition of system |
| | 3-D symmetry gives strength and damping |
| | Cubes can be summed in x,y,z for larger size boxes |
| | Fixed attachment points for 3-D mounting |
| | Defined wiring channels between cubes |
| C | Modeling Advantages (3-D symmetry) |
| | Rapid prototype models of satellite |
| | Simple and well defined x,y,z mechanical model |
| | Simple and well defined x,y,z thermal model |
| D | Electrical Advantages |
| | Common interface board (CIB) defines busses |
| | Power interface harness common |
| E | Software advantages |
| | Software defined early with common interface board |
| | Protocols for commanding and data defined by CIB |
| F | System and Schedule Integration Advantages |
| | Common shake plate and thermal vac attachments |
| | Rapid assembly and test of electromechanical subsystems |
| G | Mass Production Advantages |
| | All mechanical boxes and lids symmetrical and quantized |
| | Storage of qualified modules for rapid assembly |

III. TEST Objectives

The scientific purpose of the TEST satellite is to study how thunderstorms affect the upper atmosphere and space environment² while the engineering purpose is to validate the capabilities of a highly modular design with new technologies. Thunderstorms are known to produce gravity waves and electromagnetic energy that can penetrate deep into the space environment. Approximately 2000 thunderstorms are active near the earth’s surface at any given time, and on average, lightning strikes the Earth ~100 times/s. The average discharge radiates an intense electromagnetic pulse of ~20 Gigawatts peak power, which propagates through the lower atmosphere and into the ionosphere and magnetosphere. This energy source may produce significant variations in the earth’s global electric circuit, loss of earth’s electron radiation belt particles, communication anomalies, and density modification in the thermosphere (80-350 km) such as Traveling Ionospheric Disturbances (TIDs). A summary of the TEST nanosatellite objectives, approach and relevance is given in Table 2.

In-situ and remote sensing instrumentation on TEST will be used to study these important interactions using proven instrumentation: two 1 m Electric Field (EF) probes, a thermal plasma density Langmuir Probe (LP), a 500 Hz to 33 kHz Very Low Frequency (VLF) Receiver, two large area Solid State Detector (SSD) spectrometers for energetic particles, a 3-axis Magnetometer (MAG), a O₂ Hertzberg UV Photometer (HP), a Near UV Transient

Table 2. TEST Objectives, Approach, and Relevance

| | Science Objectives | Approach | Relevance |
|----|--|--|--|
| S1 | Understand source and propagation of Acoustic Gravity Waves into space environment (Swenson et al., 1998) | Sub-limb CCD 630nm Imager, Hertzberg Photometer, Plasma Probe | Aero braking, Ionosphere, TIDs, communication, GPS phase, D-region circulation |
| S2 | Investigate Lightning-Induced Electron Precipitation (Voss et. al., 1998) and coupling into the Radiation Belt | SSD particle detector, VLF receiver, Photometers and CCD, G. Lightning Network | Ionosphere, Magnetosphere, communication, Radiation Belt, |
| S3 | Thunderstorm Coupling to Ionosphere, heating, Quasi DC electric fields, and global electric circuit fields | Electric Field probe, Photometers, CCD imager, VLF, Ground L. Network | Ionosphere, Impulsive Parallel E fields, Weather / Ionosphere coupling, |
| | Technology Objectives | | |
| T1 | Develop a low-cost reliable nanosatellite, Include capability for several daughter CubeSat launchers for constellation studies | Based on TU Sat1 and UI IONS CubeSat, modular | Nanosatellite development, Formation flying, Reliant, Autonomous control |
| T2 | Show that a nanosatellite payload can be sophisticated and capable of new science | Advanced payload on TEST | Nanosatellites, Research, Multifunction Design |
| T3 | Develop a nanosatellite two-stage passive radiator for cooling to -60°C | Similar design to SEEP and UARS/AXIS radiators | Low Noise Detectors, Thermal Management |
| T4 | Precise attitude control for limb remote sensing on a nanosatellite | Use reaction wheels, magnetometer, magnetic torquers | Small mechanisms, Nanosatellites, sensors |
| | Educational Objectives | | |
| E1 | Stimulate many undergraduate students | Over 30 students on project, Education | New ideas!, New recruits, Creativity, Space careers |
| E2 | Stimulate secondary students and public | >100 students, Newspaper and TV coverage | Science interest, informed public, education |

Photometer (TP) and a 630 nm Imager (CCD) for airglow and lightning. In addition to the highly modular design, some new nanosatellite technology used in TEST includes a -60°C two stage passive radiator for sensor cooling, and a 0.5 degree stabilized attitude control system for remote sensing. The University of Illinois team is completing the Hertzberg Photometer and the CCD imager. The TEST measurement concept is shown in Figure 1.

IV. Satellite Instrumentation

The TEST satellite represents a suite of *in-situ* and remote sensing instruments that rival measurements on many advanced satellite systems (e.g. the DOD DMSP/POE program and the NASA Living With a Star program). New technologies and the modular design permit development of sophisticated instrumentation with modest resources. A summary of the instrument specifications are in Table 3.

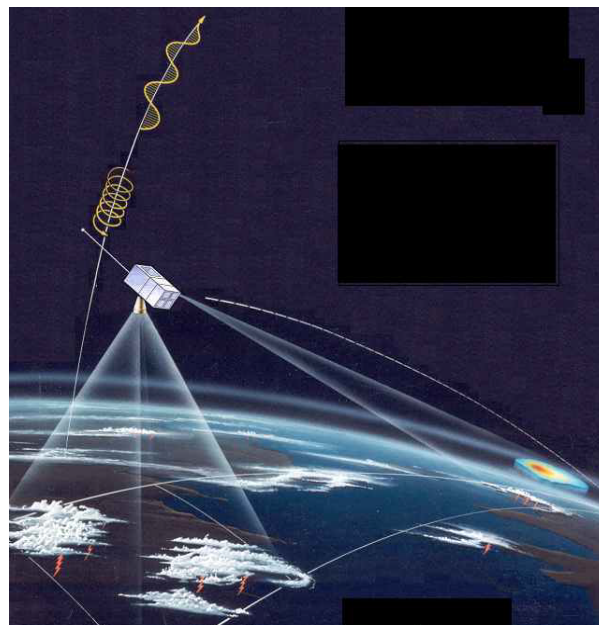


Figure 1. TEST measurement concept.

A. Langmuir Plasma Probe

The Plasma Probe mounts to the thermal shield resulting in a configuration of the probe in the ram plasma. It measures the thermal plasma density and temperature of the satellite environment. This low energy (0-6 eV) plasma probe circuit has had a design heritage on the NASA DROPPS rocket and the TU Sat 1, a CubeSat designed and constructed at Taylor University. The probe is programmable to various voltages and is connected to a log

| Instrument | Measurement | Range |
|---------------------------------------|--|---------------------------------------|
| Langmuir Plasma Probe (LP) | Thermal Electron and Ion IV curve | 0 to 6 eV |
| 3 Axis (MAG) Magnetometer | 3-Axis Magnetic Field | 40 micro-Gauss to 2 Gauss |
| Electrodynamics E-Field | 2-D Electric Field Two 69 cm booms | DC 5 mV to 1 V/m AC field to 3 kHz |
| VLF Receiver | EM Waves | 100 Hz to 30 KHz |
| Transient Photometer (TP) | UV Photons Photo multiplier | 390 nm wideband 30° FOV, dI/dt |
| Energetic Particle Spectrometer (SSD) | SSD electrons and protons | E>10 keV to E> 80 keV ions |
| Hertzberg Photometer (HP) | O2 Hertzberg Band 90 mm focal length | 260-290 nm 2° FOV |
| CCD Limb Imager Camera | 630 nm 8 deg FOV 510 pixel, 2-D image 50 mm focal length | Intensified camera 8° FOV |

provides more modularization and makes it easier for individual components to be modified without affecting the system as a whole, or creating the need for costly replacements. Figure 2 shows the SMI populated board.

B. Electric Field Probes

Two Electric Field Booms are deployed from the satellite with DC motors to provide differential voltages. The E-field circuit has an input range from 0.005 to 0.5 V/m on the vertical and horizontal plane. Similar to the Plasma Probe the E-Field circuit has design heritage on TU Sat 1, though it has gone through extensive improvements. DC voltages are passed through a filter, op-amp chain and then sampled and digitized at 20 Hz providing E-field strength information in the horizontal and vertical directions.

In addition to DC E-fields the amplified fine-structure AC variations in the DC field are also measured. By capacitive coupling to the DC output, the DC voltages are filtered out. This leaves the small AC fluctuations. The fluctuations are further amplified and then rectified by charging a capacitor in parallel with a bleed resistor. This allows for a low-sampling rate of a high-frequency signal.

C. Very Low Frequency (VLF) Receiver

The charge build-up and lightning discharge from thunderstorms produce impulsive electric fields and bursts of VLF radio energy. Ionosphere airglow observed above the thunderstorm region is associated with strong electric fields that may be important to 1) the global electric circuit, 2) the making of F region irregularities, and 3) the production of magnetospheric ducts that propagate VLF radio waves (see www-star.stanford.edu/~vlf/). Lightning-induced Electron Precipitation (LEPs) from the VLF radio waves (see Figure 1) may demonstrate a major loss of the earth's radiation belt ².

The VLF receiver responds to this electromagnetic radiation in the VLF frequency range 500 HZ to 33KHz. The VLF loop antenna, mounted to the deployed thermal shield of the satellite is tuned to the Very Low Frequency waves with the front end receiver circuit. After amplification the signal is passed through a two section, four pole, switched capacitor filter. Because of our large number of instruments and our currently limited satellite to ground throughput we are only looking at the frequencies between 500Hz to 3KHz, and 8KHz to 30 KHz.

electrometer and a low-noise instrumentation amplifier. The output of the amplifier subtracts the bias voltage and is further amplified for a 0-5 V A/D conversion. Plasma probes are common on satellites because they provide an excellent complement to the other instruments to better understand the environment the satellite is traveling through. Knowing the environment of travel provides better understanding of data from other instrumentation.

The Science Module Interface (SMI) board (Figure 2) is responsible for conditioning and amplifying the plasma probe data. Also included on the SMI board is the circuitry for two electric field probes and for a very low frequency receiver that is sensitive to lightning's electromagnetic signals. The sample rate of all instruments on the SMI board is a defined 20 Hz with capabilities of burst mode. This

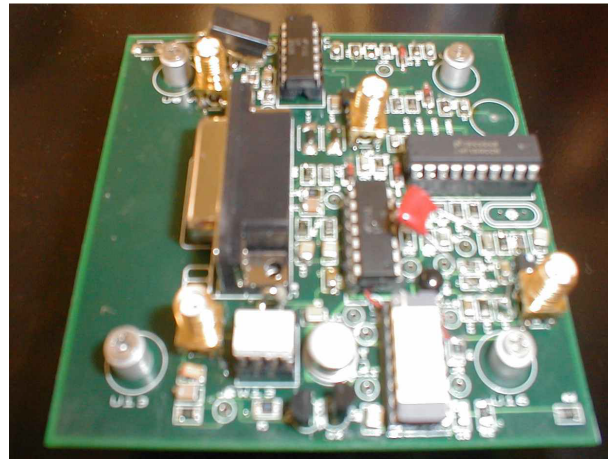


Figure 2. Common Science Interface Board.

When combined with the frequency nonspecific amplification of the circuit, the peak amplification for the center of a band-pass is approximately 2000 Hz. Following the band pass filter stage each output charges a capacitor in parallel with a bleed resistor. This allows for low-frequency digitization of the VLF wave amplitude in each of the frequency bands.

D. Solid State Detector Spectrometer (SSD)

The energetic particle spectrometer uses two 1 mm thick 0.5 cm^2 solid-state Si detector that measure electrons and ions. The detectors are mounted on the primary radiator on the dark side of the spacecraft to maintain -60° C . The sensors point 60° from zenith so that the quasi-trapped particle flux is measured. The electron detector covers the energy range 10 keV to 1 MeV and the ion detectors cover the energy range 80 keV to 2 MeV. The detectors are covered with a $40 \mu\text{g}$ aluminum deposit to make them light tight in case there is some reflection into the collimator. The field-of-view is 30 degrees. The ion detector has a 500 gauss permanent magnet in front of the collimator to sweep out the low-mass electrons. The mechanical structure is shown in Figure 4. The bottom plate shown is the primary radiator surface supported on fiberglass standoffs.

The amplified signals from the sensors are routed into a digital pulse processor (Amptek DP4) for pulse shaping and amplitude conversion. The 1000 channel pulse amplitude is directly proportional to the incident energy of the energetic particle.

E. Transient Photometer (TP)

The Transient Photometer views the nadir direction and measures light intensity vs. time. The TP utilizes a 391.4 nm filter (nitrogen line) to examine peak light emission of lighting and the aurora. After the filter an optical lens focuses the incident light into a photomultiplier tube (PMT) resulting in an amplified signal (gain 5.0×10^5). This signal is digitized, time stamped, and stored until transfer to ground. The Hamamatsu H7468 PMT (Figure 5) assembly was chosen which includes the PMT, high voltage supply, ADC, and a micro controller for serial communications. The serial output of from the H7468 is transferred directly to the TP Interface Board.

F. Limb CCD Imager

The U of I has developed a remote sensing limb CCD camera and background photometer to provide information for the study of AGWs, TIDs and Lightning (see Table 1). The OI (^1D), 630 nm emissions will be imaged in the sub-limb with an image intensified CCD camera. The field of view is 8° for limb viewing in the

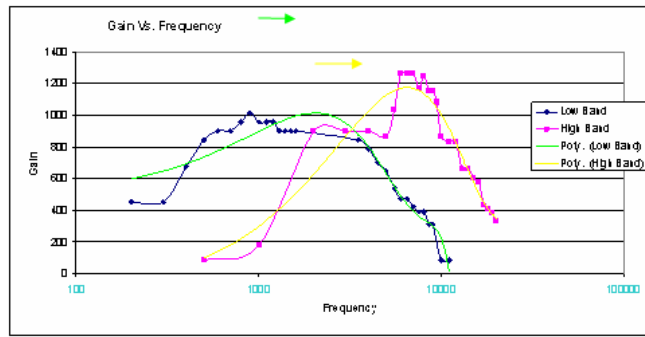


Figure 3. VLF Frequency Response



Figure 4. Ion and electron particle detectors mounted on primary radiator surface.

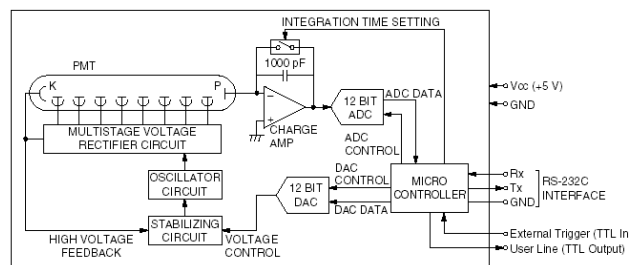


Figure 5. Logic Diagram of H7468.

orbital plane (either fore or aft). The optics are designed with $\sim f/1$ optics. The sensor is a commercially available CCD operating in either video or clocked pixels with a gated image intensifier. The sensor is optimized for light gathering at slant viewing of 200-300 R emission with a $S/N > 50$. A cold finger is thermally coupled to the passive thermal radiator that is shared with the SSD detector.

The camera consists of a 512 pixel array, and operates in two modes. The main mode is the ‘keogram’ mode, which takes a cut in the center of the image in the orbit plane providing brightness vs. elevation angle. A cut from each image is stacked for images taken every few 10’s of seconds along the path so that the brightness structure is observed. The brightness information at angles within the field of view is documented. For each ‘night’ pass, there will be one ‘keogram’ of 630 nm image cuts for study of spatial structure along the orbital path. The second mode will be a full frame mode, with infrequent full frame samples planned for targets of opportunity, such as the auroral zone. Also implemented is a background photometer for monitoring background noise.

G. Hertzberg Photometer

The second UI instrument is a nadir-viewing photometer monitoring the intensity of the O_2 Hertzberg bands in the 260-290 nm region whose emission originates near 98 km, the peak altitude of atomic oxygen density. This spectral region is shielded from lower atmospheric emissions by the ozone absorption in the stratosphere. This emission is ~ 500 R in brightness and has been observed by Swenson et al.³ with an $1/8^{\text{th}}$ meter Ebert spectrometer flown on the Space Shuttle (STS62). The nadir brightness variation due to gravity waves is typically 2-4 times the wave amplitude in temperature. Typical AGW amplitudes of 1-2% (atmospheric T^2/T) for example will have 3-6% brightness variations, the brightness variations being primarily introduced by the vertical winds associated with the waves. The system is designed to achieve a $S/N \sim 100$ with horizontal resolutions of ~ 8 km (1 sec integration time). The instruments incorporate photodiode protection circuits as well as circuit protection for low voltage.

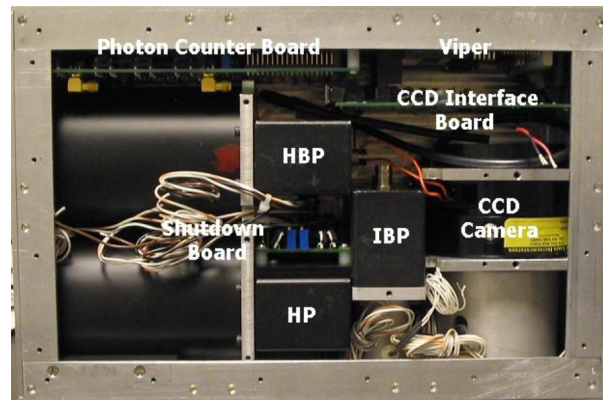
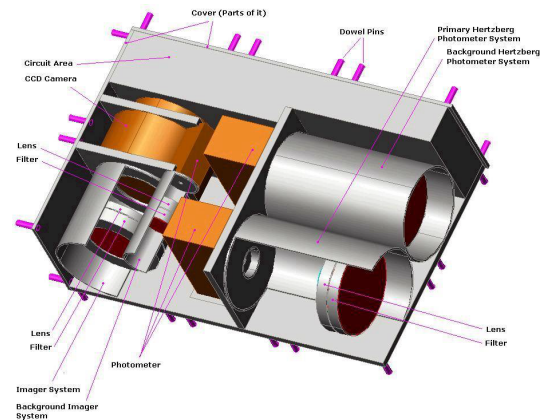


Figure 6. U of I CCD and Photometer Instruments

V. TEST MECHANICAL AND THERMAL

The constraint of a simple interface was placed upon the mechanical team so that interfaces could be defined for all of the student groups. Knowing the desire for subsystems to be easily switched out, for standardized testing, and for streamlined organization, the team was forced to consider a modular design. Because of the unique settings within a university, a simplified learning curve was needed due to the highly transient nature of student involvement. The result was a satellite where defined subsystems minimized the needed interactions between students. The CubeSat program led by Stanford University and CalPoly University¹ had already developed an extremely one dimensional modular design in which multiple universities, following precise external size requirements, could have the freedom to do whatever experimentation internal to their satellite, while not affecting others. Similar ideology was implemented with TEST where each subsystem would be isolated physically giving student engineers the

freedom to perform needed operations while not affecting others. The overall TEST satellite dimensions are 46.9 cm in diameter and 47.5 cm high.

H. Subsystem Cubes

The 4" x 4" x 4" aluminum subsystem module is the standard dimension on which the modular design rests. It provides the structural element on which PC boards are mounted, batteries are secured, and instruments are attached. Each subsystem module is capable of handling the variant environmental conditions placed upon it due to launch. Modules may be used individually for PCB stacking (custom boards defined to be 3.5"x3.5"), or be combined to accommodate unique COTS component geometries. Each subsystem module provides an effective RF shield reducing electromagnetic noise throughout the satellite. Low noise instrumentation may then be effectively isolated from noisy systems such as communications.

Each module is fastened to its neighbors through a standardized connector in the corner of each module, to form the geometry of the satellite. Interlocking cubes provide secondary support to the satellite allowing stresses to be distributed three dimensionally through the subsystem walls. Unlike traditional satellites, where load is carried through large structural panels, TEST allows for distributed loads to meet launch stresses.

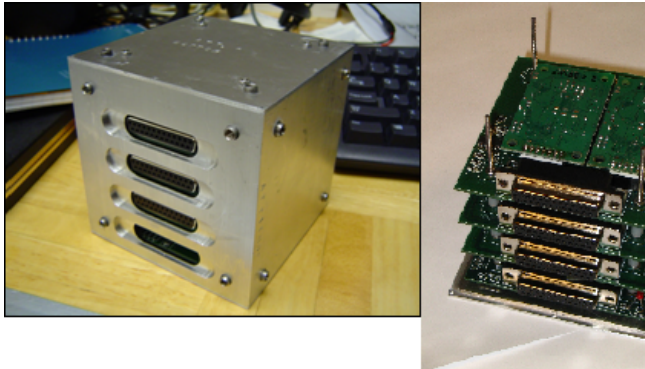


Figure 7. Attitude Subsystem Module

By stacking subsystems TEST is able to utilize all of its internal space. Each module has six walls for attaching components, allowing for efficient use of the nanosatellite package as shown in Figure 7. The flight single, dual, and the UI hex module boxes are shown in Figure 8.

The bottom deck of TEST is mounted to the nanosatellite Separation System (NSS), PSZ lightband system, and also serves as the optical bench for sensor alignment (horizon sensors, CCD imager, photometers, and attitude system).

I. Exoskeleton Structure and Solar Array

The primary structure (exoskeleton) of the satellite surrounds the assembled subsystem cubes and is responsible for shouldering the satellite load, keeping the subsystem cubes firmly attached together, and increasing the natural frequency of the satellite. The 0.5-inch thick-pocketed (weight-reduced) aluminum plates provide primary structure through vertical and lateral ribs. Attached to each wall of the exoskeleton is a 0.0625-inch sheet of aluminum acting as a shear plane to increasing the fundamental frequency at which the satellite will vibrate (first mode ~ 200 Hz). The TEST satellite in its near completed form was given a full load three-axis vibration to verify the structure and subsystem frequencies. All structural and cube primary frequencies were above 200 Hz.

Secured to the shear planes through thermally conducting standoffs are the solar arrays so that structural load is decoupled. Each solar array is constructed of a pocketed 0.25-inch aluminum sheet that runs the complete height of the satellite. Integrated to the inside of each solar wall is a magnetorquer coil that is used for attitude stabilization. The array is designed for the GaAs cells to be arranged in multiple strings. Each string consists of eight cells. Should something occur to a string each has been isolated by a diode to avoid power drains by dysfunctional strings. The solar array interfaces with the satellite through a single connector. The connector has two main positive and negative power rails within to provide redundancy in case of a power spike. Also, the connector will house two pins for the magnetorquer. The idea behind the connector is that it allows the entire solar panel to come off for testing and storage without interfering with other systems. Thus the modularity of the satellite is maintained not just within the cubes but also in the separate structures of the satellite itself.

J. Two-stage Passive Radiator

The TEST satellite includes a two-stage passive thermal radiator for cooling of satellite SSD and CCD instrumentation. The thermal radiator points facing black space away from the sun, due to attitude stabilization. The primary radiator is designed to be cooled to -60°C and the surrounding secondary radiator to -30°C . The radiator module, $4''\times 8''\times 8''$, is isolated from other modules through stainless steel connectors, reflective tape and thermal blankets. Internal to the radiator box, thermal blankets are used to isolate the second stage of the thermal radiator from the structural walls. Fiberglass tube standoffs are used to reduce heat transfer. Each wall of the secondary is polished aluminum to reflect incident solar radiation. The secondary stage is designed maintain an average temperature of approximately -30°C . The primary radiator is isolated from the secondary by fiberglass standoffs and is painted black for high emissive radiation. Design objective for the primary is to average -60°C .



Figure 8 - Flight single, dual and hex modules (without exoskeleton walls)

K. P-Pod Launcher for two dual cubes

The primary assembly for the satellite shown in Figure 8 consists of space for $3\times 3\times 3$ cube matrix. Above the matrix is space for mounting two CubeSat dual P-pod launchers⁴. The P-Pod launcher, developed by California Polytechnical State University, is capable of launching 4 cubesats independently from the TEST Satellite. With the main satellite mechanically isolated from the P-Pod launch system instrumentation, the modularity of the satellite is maintained. An IDEAS model of the satellite is shown in Figure 8.

L. Thermal Model

The modular subsystem design with an exoskeleton structure is ideal for meeting the various thermal requirements placed upon a satellite. The exoskeleton walls, as well as the subsystem modules, act as thermal shorts between the illuminated side of the satellite, and the side facing black space. Each subsystem conductively transfers its thermal energy through its Al walls, and the walls of its neighbors to the cold side of the satellite. Black anodized modules allow for thermal transfer through radiation as well. Thermal isolation of each module is obtained by using thermally insulated attachments when assembling the cubes, and/or placing thermal blankets between cubes. An IDEAS Thermal model of the TEST satellite is shown in Figure 9.

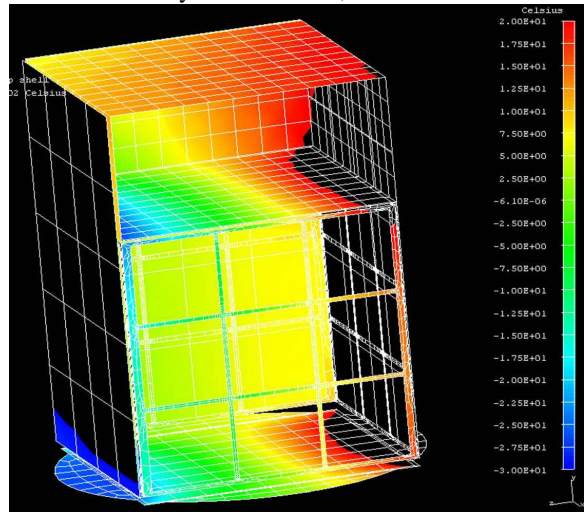


Figure 9. IDEAS modular thermal model

M. Deployables

Due to the various requirements of several scientific instruments being flown, the TEST satellite needs the capability to deploy sensors, with precise knowledge of boom placement relative to the satellite body. TEST will deploy two electric field booms, and one thermal shield as shown in Figure 10. All deployables are located on the radiator side of the satellite and are mounted to a single shear plane. This allows for complete deployment testing independent of exoskeleton and subsystem module construction and does not interfere with the solar panels.

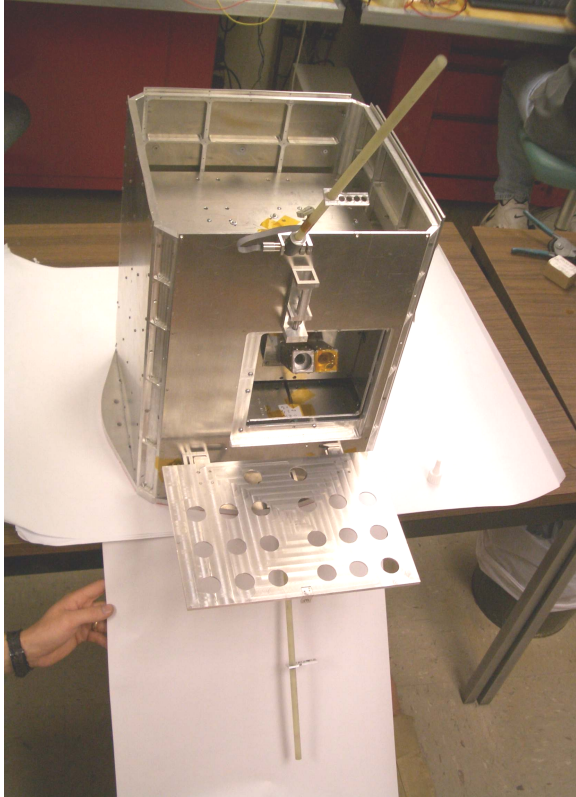


Figure 10. TEST Deployables

The Electric-Field booms are constructed of hollow-core fiberglass rod connected to a custom hinge on one side, and a gold plated aluminum sphere on the other. An RG-174 cable runs from the aluminum sphere, inside the fiberglass rod, and to the science module. The E-Field Booms are deployed by two 14 oz DC motors with a gear reduction of 1024:1. A digital encoder secured to the shaft of the motor outputs two pulses per revolution providing excellent knowledge of deployment distance. Each boom will be ~18 inches and will hinge from opposite corners of the radiator side shear plane, opening along the vertical

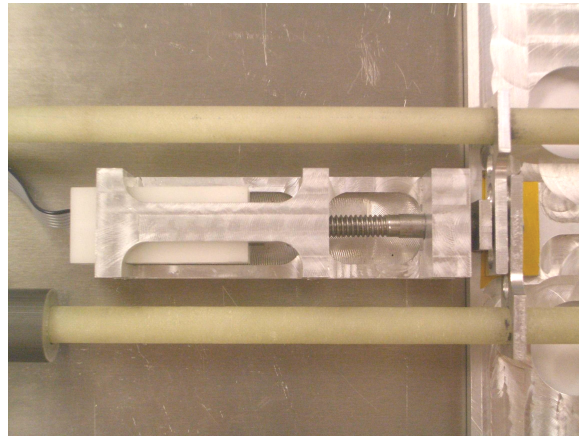


Figure 11. DC motor Release Mechanism

axis of the satellite. This provides a tip-to-tip distance of ~54 inches. Fastened to one of the booms is a Honeywell three-axis magnetometer providing attitude knowledge.

The E-Field booms, being long and flexible, need to be held in place during launch. Many COTS release mechanisms pose too high of a cost for our application, so designing our own mechanisms proved to be more cost effective. The release mechanism utilizes a DC motor with a digital encoder and a 1024:1 planetary gearhead, housed in Delrin. The Delrin is fixed in two axis, and is able to slide freely along the third inside an aluminum housing (see Figure 11). The shaft of the output shaft of the gear head is fixed with a pin to a customized pin that is smooth on one half and threaded on the other half. As the motor shaft turns it unscrews the pin, pushing the motor backwards, and releasing the confined E-Field booms.

When all the deployables are in a stowed position, the E-Field booms lie across the thermal shield, and serve to secure the shield in place during launch. After the E-Field booms have been released and deployed the thermal shield is free to be deployed as well. The thermal shield is protecting the two-stage passive radiator from incident radiation of the earth's albedo and emission. The shield is constructed of polished aluminum on the top and Optical Solar Reflective (OSR) tape on the bottom. A DC motor identical to the ones used by the E-Field booms rotates the shield into place. The shield also serves as a mounting platform for a plasma probe and VLF antennae. The plasma probe will measure the thermal plasma density of the spacecrafts environment, and the VLF will record very low frequency waves produced by lightning and radiation belt hiss.

VI. ELECTRICAL SYSTEM

N. Wire Harness

One of the most exciting and innovative designs of the TEST Satellite is the standardization of the wire harness. Each connector external to a module has been standardized to be a 9, 15, or 25 pin D-Subminiature connector, and low-noise instrument wires have been standardized to an SMA coax connector. These easily accessible, flight heritage connectors provide reliable connections from the various subsystems. Each subsystems external connector is then connected to a central routing printed circuit board (Mother Board). Complex multi-subsystem connections can be made with the ease of PCB routing technology, greatly reducing spacecraft wiring difficulties. Typically each subsystem would require one cable from the Mother Board to the subsystem, though multiple connectors are easily added. Though the use of D-sub's in space is hardly a new practice, the combination of highly reliable connectors combined with a centralized routing PCB complements the Nanosatellite package well.

The Mother Board has been designed to assist in simplifying the complex wire harness TEST would have required. It was also designed to assist in subsystem testing once the spacecraft has been designed. Diagnostic wires defined by each subsystem team are accessible through connectors placed on the Mother Board that monitor subsystem functions. LED's have been placed on defined functions telling the designer whether power is on, microcontrollers are functioning, or other procedures are functioning as planned. Through this added feature satellite system testing will be reduced, giving a better understanding of satellite functionality and subsystem particularities. RF pick-up, magnetic interference, or other disturbances caused by nearby subsystems may be better diagnosed. Also available on the Mother Board is the ability to program subsystem microcontrollers. Each microcontroller (described later on in paper) has a programming connector placed on the motherboard for reprogramming subsystem Microcontrollers.

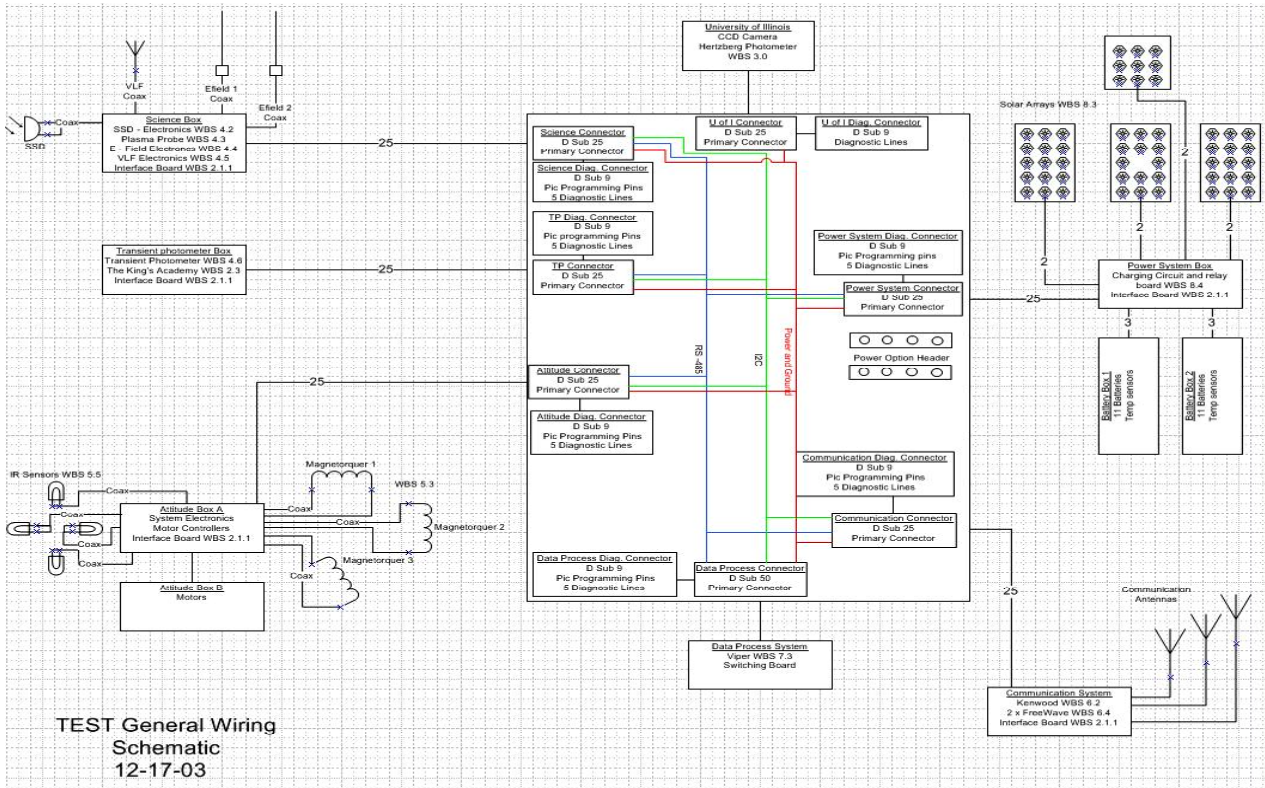


Figure 12. Wire Harness Logic Block Diagram

Another benefit in the TEST wire harness is that subsystem cables have been defined so that common electrical functions are performed on the same pin number. This allows for efficient system testing and helps prevent crossing wires when creating the wire harness. The wire harness system diagram is shown in **Error! Reference source not found.**

O. Common Interface Board

Throughout a satellite many components perform the same operations, but for different subsystems. Responding to this inefficiency the TEST satellite has taken a large number of common subsystem functions, and standardized them within a single printed circuit board, called the Common Interface Board. The Interface Board is the bridge between the instruments, the attitude control, the power control, the communications, and the rest of the satellite. The common interface board is shown in Figure . Functionally this board has a PIC18F8520 microcontroller, 512 Kbytes of non-volatile RAM, three high current solid state detector relays, three low-power current sensors, a -55°C to 130°C temperature sensor, buffered analog to digital lines, I/O lines, and LED's for determining subsystem performance during testing.

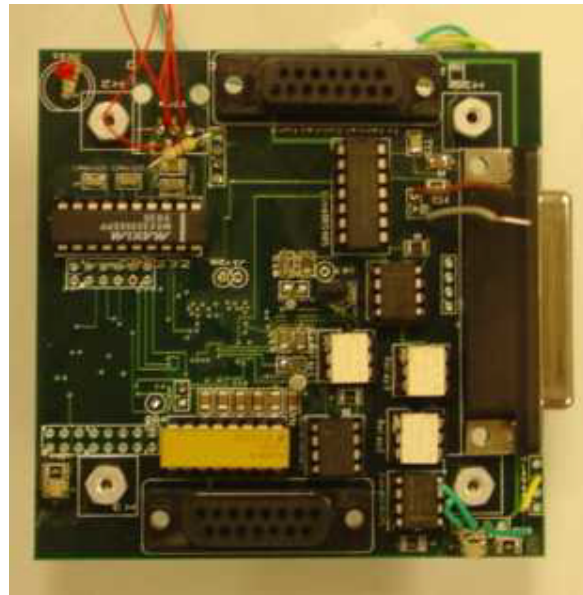


Figure 13. Subsystem Interface Board

The PIC18F8520 acts as operations manager for each subsystem, turning subsystem components on and off, collecting instrument data, and monitoring various health and diagnostic information. The microcontroller has 68 I/O lines, 16 A/D lines, and 2048 Bytes of ram, though only 7 A/D lines and 8 I/O lines are available for subsystem use (an additional 33 I/O lines are available if the 512 Kbytes of RAM is not used). Each microcontroller is programmed to fulfill the various needs of the subsystem. Each subsystem PIC communicates to the satellites central On Board Computer (OBC) over an RS485 bus with a back up I²C bus. In addition to these external communication buses the Interface Board provides an RS232 and Dallas 1-wire bus for all internal instrumentation. This allows instrument designers the ability to collect data through analog signals, or by using COTS where data output is a standard RS232 or 1-wire interface.

From a safety perspective the interface board acts as buffer from relatively unpredictable subsystems, and the satellites critical main board computer. Each Interface Board is designed and ruggedly tested to protect the RS485 data bus and prevent bus latch ups. Mechanically the Common Interface Board fits the predefined 3.5" x 3.5" cube space. Reliable D-Sub connectors allow for subsystems to stack PCB's on top or connect through a wire harness.

P. Power System

TEST employs a power monitoring and control system that is capable of handling the various requirements placed upon it by the large number of instruments, two onboard flight computers, two communications systems, and an active attitude control system. The system was designed with modularity in mind as it was the deciding factor to split the power subsystem into the following 5 discrete circuit boards: microprocessor, charging, voltage regulation, power distribution, and solar peak power tracking. A power system diagram is shown in Figure . The power control system is housed in a single 4" x 4" x 4" cube and consists of the four custom PCBs and one Interface Control Board.

The relay must be magnetic latching instead of solid state to ensure that if the state of one set of contacts changes, the other set of contacts will also change to a different state. These inhibit verification lines are passed through the external 25 pin D-sub connector to the Electrical Ground Support Equipment (EGSE) connector for ground testing. The solar connection used for battery charging and direct energy transfer (DET) to the load is made through 15 pig-tailed lines that interface with the solar peak power point tracker via a 15 pin D-sub connector. The micro switch connections are included in this wire harness because they act as the ignition mechanism to connect the solar array to the power bus. This board implements a "star" ground topology by placing the analog ground connection at a single point nearest the battery ground. Both the analog and digital grounds are kept separate throughout the rest of the satellite and return to this single point, effectively minimizing unwanted voltage drops and ground loops. The final output of this board is an unregulated voltage line, digital ground, analog ground, four I/O

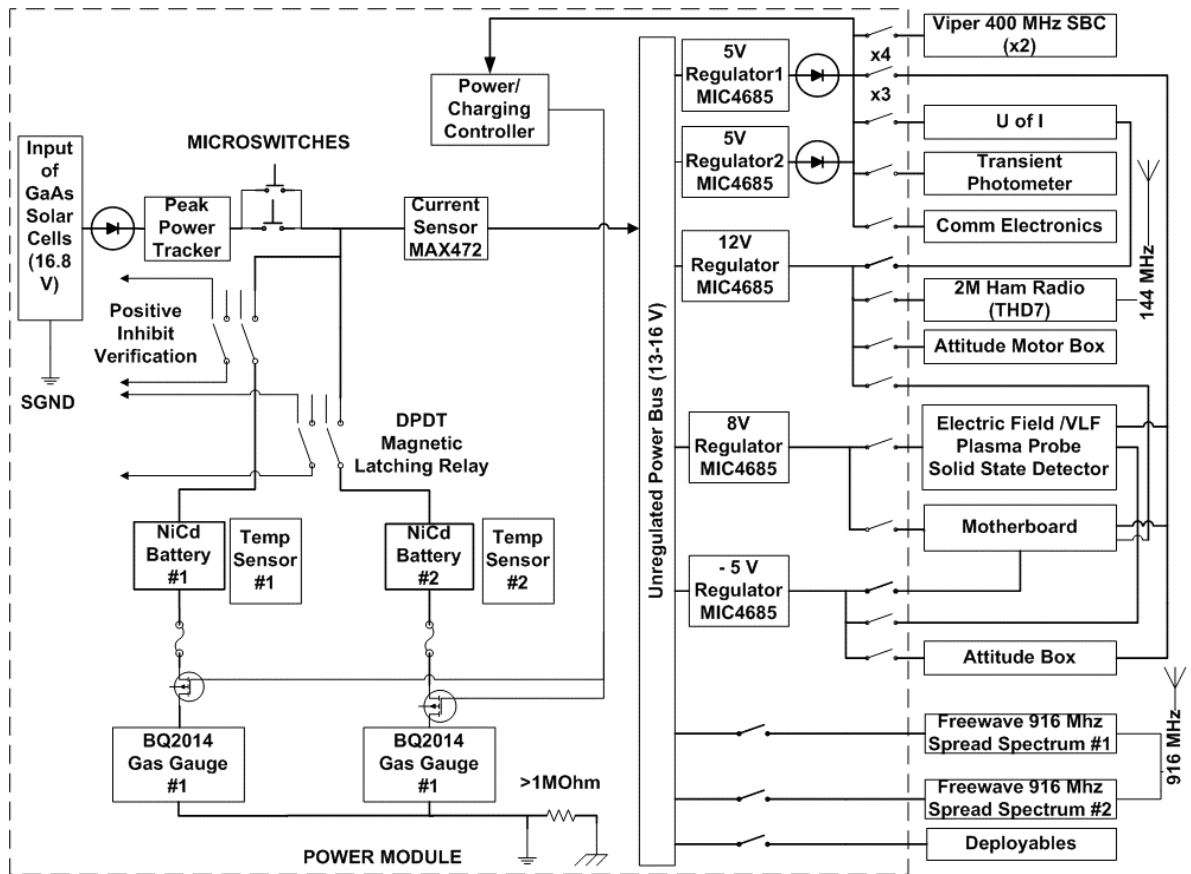


Figure 14. Power System Diagram

lines, and two Dallas 1-Wire busses, which are passed to the voltage regulation board. A second 1-Wire bus has been created to allow for redundancy in the case that a short occurs on one of the busses.

The second power board is the voltage regulation board, which takes the unregulated power line from the first board and passes it through 5 separate voltage regulators to provide the various voltages needed in the satellite. The following voltages are provided to all subsystems: -5, 5, 8, 12, and unregulated. The MIC4685 switching regulator in a step-down configuration is used for all five of the voltage regulators due to its ability to support 3A of current, its relatively high 85% power efficiency, and previous experience with the MIC family on TU-SAT1. Extra storage capacitors were added on each regulator to ensure that the voltage remains rock solid. A MAX471 current sensor is placed on each positive voltage line and then connected to a DS2450. Voltage dividers are also used to monitor all of the positive voltages. Due to the lack of A/D converters that accept a negative voltage input, only the current through the -5 V rail is monitored by a MAX4172 current sensor. In order avoid single point failures and increase redundancy, a second 5v regulator was added and tied to the primary regulator with Schottky diodes. In the event that either 5v regulator fails, the other regulator will still provide power to the 5v bus. This was necessary due to the large amount of microcontrollers and flight board computers that require 5v to operate. The final output of this board are 5 voltage busses, 2 1-Wire busses, digital ground, analog ground, and four I/O lines, which are passed to the power distribution board.

The third board on the stack is the power distribution board, which takes the five regulated voltages and passes them through solid state relays to each of the subsystems. Every line out of the power subsystem is inhibited by a PVN012 relay. The PVN012 is a 4.5A solid state relay that requires only 3mA for operation and has a low on-state resistance of 40 mOhm. In order to switch the 20+ output lines on and off, many IO control lines were needed. The 1-Wire DS2408 switches were used because they supply 8 I/O lines through serial command over the 1-Wire bus, which reduced the wire harness and did not require the use of multiple D-latches. In order to guarantee that the Viper computers power up, each output is controlled by two relays in parallel. One of the relays is controlled by one of the PIC I/O lines, while the other relay is controlled by an I/O line from a DS2408. The remaining two PIC I/O

lines were used to control the Freewave radio relays. Before leaving the switching board each subsystem power line is passed through a resettable poly-fuse. Fusing the outputs ensures that the regulators will not be damaged and also protects the wiring and PCBs. Resettable fuses are used in the design to prevent a subsystem from being permanently cut off from the satellite in the event of a voltage spike or a short burst of high power draw. The power subsystem monitors the final subsystem 5v output voltages via a DS2450 to ensure that a subsystem is actually on.

In the event that the I/O line controlling the relay is high and the fused output is low, the PIC can reset the fuse by turning the relay off and then back on. The 5v lines are monitored due to the ease of being able to directly connect them into the DS2450. Also, only the 5v lines were monitored because they are the most important due to the fact that they supply power to the microcontrollers and Viper flight computers. In another attempt to minimize single point failures, roughly half of the relays are controlled by DS2408 switches on 1-Wire bus A and the other half by 1-Wire bus B. The subsystem voltage outputs were split up in such a way that if 1-Wire bus A shorts, the satellite will still have an operational mode with the outputs controlled by 1-Wire bus B.

The last board on the stack is the solar peak power tracker board (Figure). This board has a 15 pin D-sub connector that contains the positive and negative connections for all four of the solar panels. There are two sets of positive and negative connections per panel for redundancy, except for the top panel which provides less power than the other three panels. Since every string has a blocking diode placed on the solar panels, this board does not need to have blocking diodes onboard. The current provided by each panel is sensed by a MAX471 and all of these are connected to a DS2450. The panels are all then tied together as one line that is connected to a step down switching regulator. This regulator has its feedback off of the input voltage to hold the solar array at a specific voltage, the max power point. Since the maximum power point for the array will be dynamically changing due to the panels being on different axes and changing temperatures, a digital pot is in the feedback divider for the PIC to continuously search for the peak power point. The input voltage and the output voltage are both sensed via voltage dividers.

The output voltage, called the peak power voltage, also has a MAX472 current sensor for system monitoring. Two MOSFETs are placed in parallel between the negative connection of the solar array and the solar ground to inhibit power flow from the solar array to the satellite subsystems. These MOSFETs are driven by a MOSFET driver to ensure that the array is fully on or fully off. The gate of the MOSFET is driven by the total solar voltage only after the satellite is deployed from the Internal Cargo Unit (ICU). This mechanism is based on two micro switches in parallel that are open circuit during compression in the ICU. Once TEST is deployed, the switches become a short and apply the solar voltage to the gate of the MOSFETs, effectively connecting the solar array to the satellite power bus. This board connects to the charging board through a 15 pin D-sub connector.

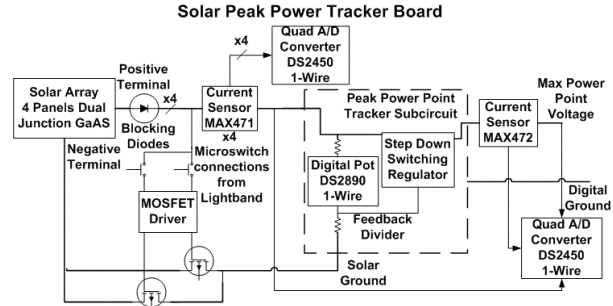


Figure 15. Solar Peak Power Tracker

VII. ATTITUDE CONTROL SYSTEM

The TEST satellite requires 3-axis attitude stabilization within 1 degree of its target orientation. Rarely seen in nanosatellites, such stabilization will allow for a much greater range of instrumentation and experiments to be flown on the nanosatellite platform. For TEST the pointing capabilities of this accuracy are required for the CCD camera, which views the limb of the earth. Likewise, attitude knowledge is required for the three photometers, the solid-state detectors, and the communications subsystems.

In order to meet these specifications, TEST implements a reaction wheel system with magnetic torque coils for momentum dumping. Attitude knowledge is determined using two infrared horizon sensors and two three-axes magnetometers. The horizon sensors provide knowledge along the pitch and roll axes, while the magnetometers provide knowledge along the yaw axis and redundant knowledge along the pitch and roll axes. Deterministic methods are used for attitude determination. There are no gyroscopes on TEST, so rate estimation is accomplished by comparing successive magnetometer measurements. The control flight software is run on a dedicated onboard computer, while a custom micro-controller interface board controls all hardware functions. The interface board and the onboard computer are interfaced through an RS485 bus. The TEST attitude system is shown in Figure and electronics module in Figure .

Digital to analog and analog to digital conversions are performed on a series of custom boards housed within the attitude control electronics module. Also housed within this module are the custom micro-controller interface board and four COTS motor controllers used to control the four reaction wheels. A second attitude module houses the reaction wheels, three of which are oriented along the three primary axes and the fourth of which is skewed relative to the others. By housing these electromagnetically noisy components in their own Faraday cage (AI module), sensitive A/D measurements can be performed within close proximity of this module. Desaturation of the reaction wheels is made possible by running current through three magnetic torque coils. Countering torques allow the satellite to remain stable during desaturation. The magnetic torque coils are located on the solar panels for maximum surface area and are capable of bi-directional current flow.

System Diagram

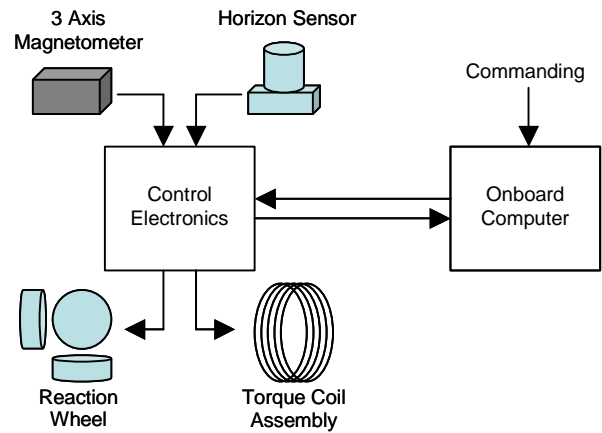


Figure 16. General Attitude System Diagram

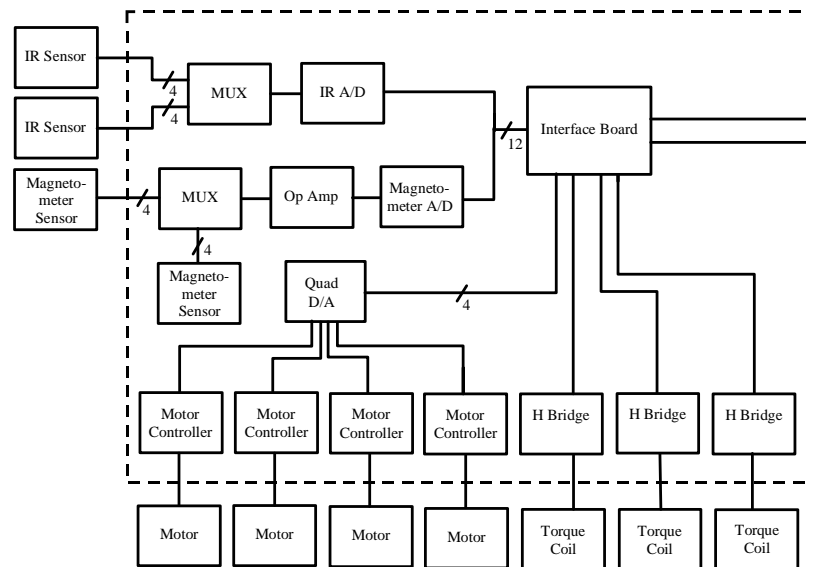


Figure 17. Attitude Electronics Control Module

Control of the attitude system is accomplished by continuous feedback communication between the control software and the attitude hardware as shown in Figure . First a target orientation is uploaded to the determination software on the attitude computer. The target orientation is then compared with the actual orientation given by the attitude sensors. A corrective translation is computed and a rotation command is input to the controller.

The controller computes the appropriate actuator commands and sends them to the interface board. The interface board commands the reaction wheels and torque coils. Finally, sensor data collected by the interface board is output to the onboard computer for feedback verification.

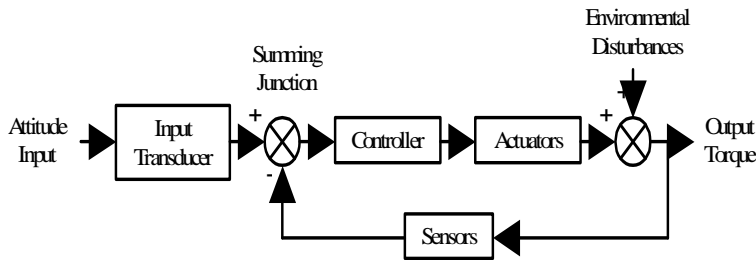
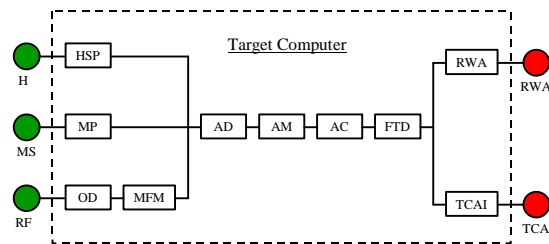


Figure 18. Basic Control Loop

Using the flexible programming environment of Matlab, a disturbance model was first created to emulate the spacecraft environment. This model includes such environmental forces as solar and albedo radiation and aero-drag. A model accounting for the specific physical properties of the TEST satellite was also created for use by the disturbance model and other simulation modules. Orbit simulation will be completed in Simulink, and prototyping of the control system will be done using the xPC Target kernel developed by Mathworks. Determination algorithms for the infrared horizon sensors are being provided by Optical Energy Technologies. All other algorithms will be written in-house using Matlab and Simulink.

Perhaps the most exciting aspect of TEST's attitude determination and control system is its modularity. Because of the unique mechanical and electrical constraints placed upon all of the satellite subsystems, the attitude system has proven to be extremely versatile. Its modular design allows it to be easily integrated with almost any satellite bus with little modification. Furthermore, actuator and sensor hardware are easily replaceable and can be custom designed for any specific mission objectives. Using the same design strategies, a fully customizable attitude system for commercial and scientific nanosatellites would be very feasible. The electronics module makes this possible. By strictly defining sensor, actuator, and computer interfaces, such peripherals could be exchanged at will making hardware development simply a matter of connecting modules. Furthermore, using Real Time Workshop and xPC Target in conjunction with Matlab allows the user to place embedded control software on almost any processor. Simulations can be done in real time using actual flight processors extremely early in the development stage allowing for simultaneous development of the attitude software and hardware. This is accomplished by simulating the attitude hardware on a standard PC and communicating with the satellite processor through the xPC kernel. Because all the sensors and actuators are first simulated in Matlab, transitioning from the simulated environment to the actual environment is relatively easy. Thus the array of options available to the attitude engineer is made extremely broad and cost effective.

The flight software and simulation software for the TEST attitude system are currently being developed at Taylor University using the Simulink environment provided by Mathworks. The flight software will eventually be compiled onto the onboard computer using Real-Time Workshop and xPC Target. To simplify the design process the Spacecraft Controls Toolbox, developed by Princeton Satellite Systems, was relied upon heavily.



Note: Sensors and actuators may be modeled in Matlab

Diagram Key

- | | | |
|---------------------------------|-----------------------------|--|
| HS = Horizon Sensor | OD = Orbit Determination | FTD = Force & Torque Distribution |
| MS = Magnetic Sensor | MFM = Magnetic Field Model | RWAI = Reaction Wheel Assembly Interface |
| RF = Radio | AD = Attitude Determination | TCAI = Torque Coil Assembly Interface |
| HSP = Horizon Sensor Processing | AM = Attitude Maneuver | RWA = Reaction Wheel Assembly |
| MP = Magnetometer Processing | AC = Attitude Control | TCA = Torque Coil Assembly |

Figure 19. Top level flight software architecture

VIII. COMMAND AND DATA HANDLING

The command and data handling system of TEST, and the software associated with it, has been designed to complement the high degree of modularity offered by the mechanical system. The software will be addressed in the next section. The command and data handling system of the satellite can be broken up into three logical levels: the microcontroller level, the Single Board Computer (SBC) level, and the ground station level.

A microcontroller is located on the common Interface Board of each subsystem and is connected to one or more instruments via connections and hardware on the Interface Board. The connections provide up to six analog-to-digital conversions, an RS-232 serial interface, and a one-wire serial interface. Through these interfaces, the

microcontroller on the Interface Board controls and collects data from the instruments, storing the data on 512 KB of SRAM external to the microcontroller. The Interface Board and the microcontroller on it are also used for the attitude control, power, communications, and deployables systems. An I²C bus allows for communication between each microcontroller, while a RS-485 serial bus provides a connection to the SBC level. The I²C bus is also a redundant bus for communication with the SBC level.

The central computing of the satellite is performed by two low powered (280 mA) SBCs called Vipers that are manufactured by Arcom. Each Viper features an Intel PXA255 400MHz processor with 64 MB of SDRAM and a CompactFlash drive with capacity of 1 GB. Each SBC runs a version of embedded Linux developed by Arcom and comes with 5 USART serial ports (four RS-232 and one RS-422/RS-485) and 16 digital I/O ports. The Viper was modified to allow access to the I²C bus.

On the functional level, one Viper is responsible for data collection from all instruments and transferring it to the ground via the communication system. Communication with the microcontroller level is performed via an RS-485 bus with an I²C bus for redundancy. The RS-485 bus is full duplex, allowing for simultaneous transmission and reception, and has the capability of connecting up to 256 devices, which provides a large amount of expandability and modularity. A new microcontroller can be added with relative ease by providing the Viper with its address. The only instruments not using the Interface Board are the U of I instruments. The U of I module is using a third Viper and a microcontroller to collect data from its instruments. Communication with these processors takes place over two full-duplex RS-232 connections. Communication with the radios on both the satellite and the ground station also happens through a RS-232 connection.

The second Viper is dedicated to the attitude system for performing higher-level orbital computations and is connected via separate RS-485 serial and I²C busses to a microcontroller on an Interface Board for the attitude system. This Viper also has the ability to communicate with the ground through a separate radio for redundancy. In case of a serious malfunction of either Viper, the other Viper is able to connect the two RS-485 busses and the two I²C busses together by closing the bus switch and thus take over all satellite operations.

The final level of the command and data handling system is the ground station level. This level, in terms of hardware, simply consists of a Pentium III computer running Linux with a RS-232 serial connection to a 900 MHz radio. This computer is responsible for communicating with the satellite every time the satellite is overhead. This communication consists of downloading data and uploading various commands.

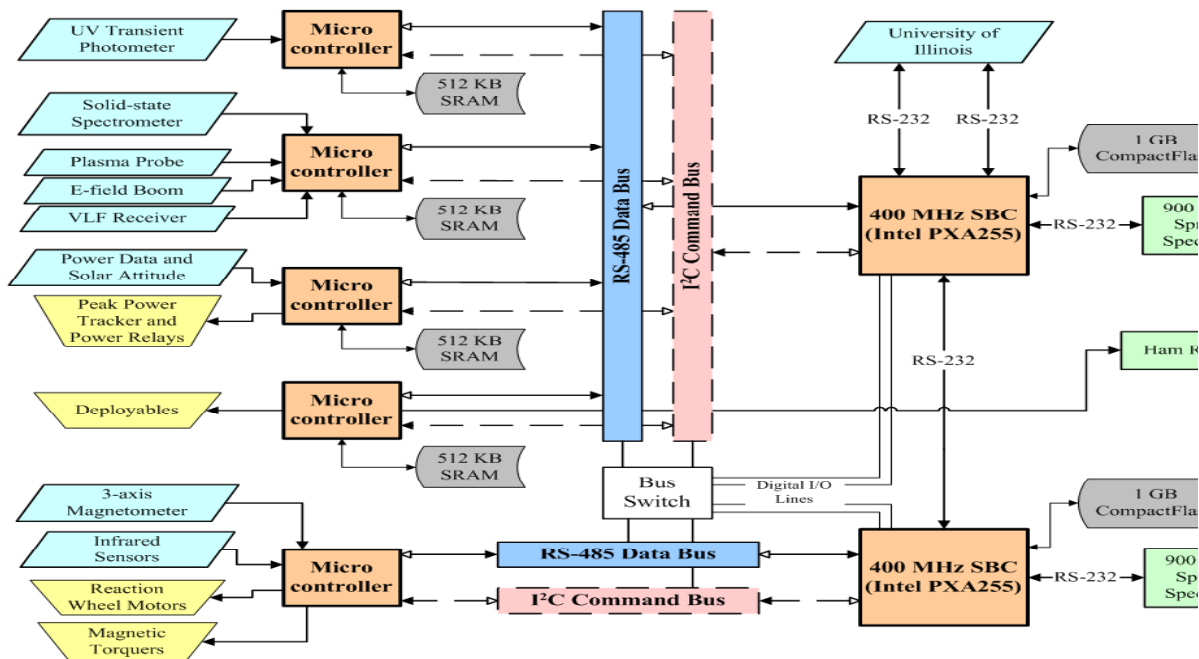


Figure 20. Processor system

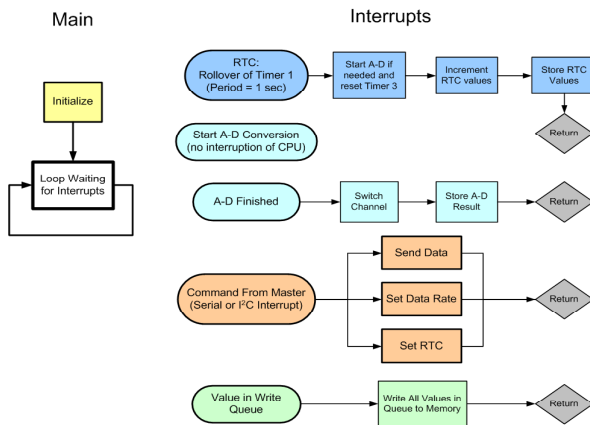
The overall layout of the command and data handling system can be seen in Figure 1. The microcontroller level is on the left; the busses are in the middle, and the SBC level is on the right. The ground station level is not shown because of its simplicity.

Modular Software System

The software associated with the hardware of the command and data handling system is a vital part of the satellite. The software is also modular, complementing the modularity of the mechanical system. The software can be viewed from the same three logical levels: the microcontroller level, the SBC level, and the ground station level.

On the microcontroller level, many common software functions have been standardized to form libraries that can be replicated throughout the subsystems. These functions have been grouped by their applications, which include a real time clock, analog-to-digital conversion, external memory access, one-wire communication, communication with the SBC level, and a variety of other applications. By creating these libraries of functions, coding and debug time is greatly reduced while dependability of the software increases. Each subsystem also needs some unique functions or some slight variations of an existing function. Thus, the code must be customized to work with each subsystem. Most of these changes are slight, however; leaving most of the code located in the libraries. Since the microcontroller is interrupt driven, a new function can be easily added as another interrupt. A flow diagram of a simple microcontroller program showing the four main interrupts is shown in Figure 2.

The SBC level has two main sections of software: one for communication with the microcontroller level and one for communication with the ground station level. The main goal of communicating with the microcontroller level is to retrieve the data collected from the instruments.



Each microcontroller has its own address and is polled periodically by the data collection Viper. Then, a simple protocol is used to transfer the data. After initial handshaking, the microcontroller sends a block of the data and the Viper acknowledges reception, and this repeats until all the data is sent. The Viper then performs compression (gzip and tar) on the data and stores it until contacted by the ground.

The other section of software on the SBC level communicates with the ground station level. A program called serial transfer protocol (STP) controls this communication. On either side of the communication, interface programs are

Figure 21. Top level flight software architecture

responsible for initiating STP and then controlling what is transferred through the connection.

In keeping with the modular design of TEST, the satellite's software is logically separated into several files. Both STP and all the interface programs are built around a number of modules containing logically related functions, providing for easy inclusion in the communication client and server. The relationship between the modules can be seen in Figure 3. Additionally, STP and the interfaces are themselves separated into several functions. This serves to keep the code modular and easy to read. The main function of each of the communication programs can be understood as a series of function calls.

STP is the program used to establish a connection and control the communication between the satellite and ground. It is designed to establish a guaranteed error-free transmission channel over a serial connection. It splits data into packets, and uses a sliding window protocol to guarantee successful transmission of all packets. It is connection-oriented, returning an error if the connection is interrupted and all data is not sent.

STP can be run in two modes: server and client. Running in the server mode on the satellite, STP remains in a passive mode until a client initiates a connection. The connection is considered active as long as both sides have received some sort of input within a given window of time. If run as a client from the ground station, STP attempts to initiate a connection, and returns if unsuccessful. If the connection is broken at any point, both client and server return.

The interface Satsrv (SATellite SeRVer) is the program run on the data collection Viper of the SBC level. Satsrv initiates and maintains a STP session in server mode. Additionally, it contains a list of all possible commands that might be sent through STP from the client side, and code to retrieve and carry out each command. The commands available through Satsrv provide complete control of the satellite from the ground station. Finally, capability exists to upload new command plug-ins for the server after launch, or even a new STP or Satsrv executable.

On the ground station level, STP is run in the client mode. On the client side, the software is further modularized into several small, but useful, utilities. The first of these is SatShell, the Satellite SHell. The onboard SBCs run an embedded version of the

Linux operating system, which can be accessed through a command-line interface known as a shell. SatShell is designed to use the STP program to transfer this shell interface to the ground station. In this way, one can gain complete control of the satellite from the ground while a radio link is available, allowing one to perform any task – including remote reset of the onboard systems, if necessary. SatShell also provides the user an option to recover if a program hangs the system. The user can reestablish a connection and end the offending program. A special packet type, designed to perform this task, is included in the serial transfer protocol.

The next utility in the modularized client software package is Satftp. This program includes the core functionality originally intended for the client/server architecture. Its purpose is the transfer of files to and from the satellite. Using this program, data collected on the satellite can be retrieved to the ground, and new software or configuration files can be uploaded to the satellite. The importance of this utility is that ANY onboard software system can be upgraded in this fashion – even the core operating system, should it be required.

The purpose of the SatTime utility is to update the onboard clock of either SBC. The time can either be passed as a command-line string, or the current system time can be uploaded. The last utility in the package is SatEcho. It is a ping utility; its sole objective is to ascertain that communication is established. It simply sends up a string to the server. If the server echoes the string back, communication can successfully be established. If it does not, a connection cannot be established.

IX. COMMUNICATIONS

The TEST satellite uses a combination of a proven, reliable transceiver and an experimental higher data-rate transceiver. The flight heritage transceiver flying is a TH-D7 dual band amateur radio. The TH-D7 has a built in TNC allowing for serial connection from the communications module microcontroller directly to the radio. The amateur radio will be primarily used for transmitting a beacon with health and diagnostic information. This radio will be utilizing the standard AX25 protocol allowing amateur radio operators around the world the capabilities of listening to the satellite as well as posting the satellite’s health information online.

The higher-data rate transceiver being flown on TEST is a COTS 900 MHz spread spectrum transceiver produced and distributed by FreeWave Technologies (Figure). Utilizing a proprietary hop table on an international frequency this COTS has excellent signal to noise ratio (-106 dBm sensitivity) allowing for lower transmit power while maintaining excellent data transfer. FreeWave also performs buffered 32 bit CRC transmission with notification when connection is lost. The 900 MHz FreeWave is capable of ~115 Kbps of continuous throughput. Extensive testing has been performed on the FreeWave transceiver through Eleven High Altitude BalloonSat

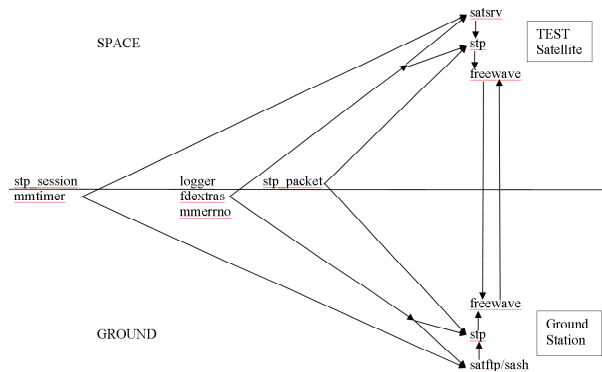


Figure 22. Software Module Links



Figure 23. COTS spread spectrum 900 MHz transceivers

Launches here at Taylor University. During these flights in which the FreeWave was carried to heights of 100000 ft and ~115 miles away from the ground station, high-data rate communication was kept throughout the flight.

The FreeWave is directly connected to the Viper through an RS232 line bypassing the communication microcontroller. A second 900 MHz FreeWave is housed in the communication module and is connected to the Attitude Viper in case of failure of the primary FreeWave or primary Viper.

The communication module is made of a double cube and houses the two FreeWaves and the TH-D7. The module also houses the Communication and Deployable Interface Board. This dual function Interface Board functions as the director for the deployments immediately upon insertion into orbit. Once this is complete its sole purpose is to collect health and

diagnostic information received up on the I²C bus and transmit it through the TH-D7.

X. BALLOON LAUNCH

One of the main objectives of the TEST satellite is to emphasize testing of subsystems for burn-in and qualification. In addition, end-to-end testing is needed from instruments, to processors, to software, to communication link, to ground station, and to data analysis, and finally to calibration. In the past year and half Taylor University has successfully launched 12 balloon payloads to altitudes above 25 km where the near space environment is experienced (UV and 1% atmosphere). In addition the link margin can be tested over 100 miles. A block diagram illustrating the balloon launch configuration is shown in Figure .

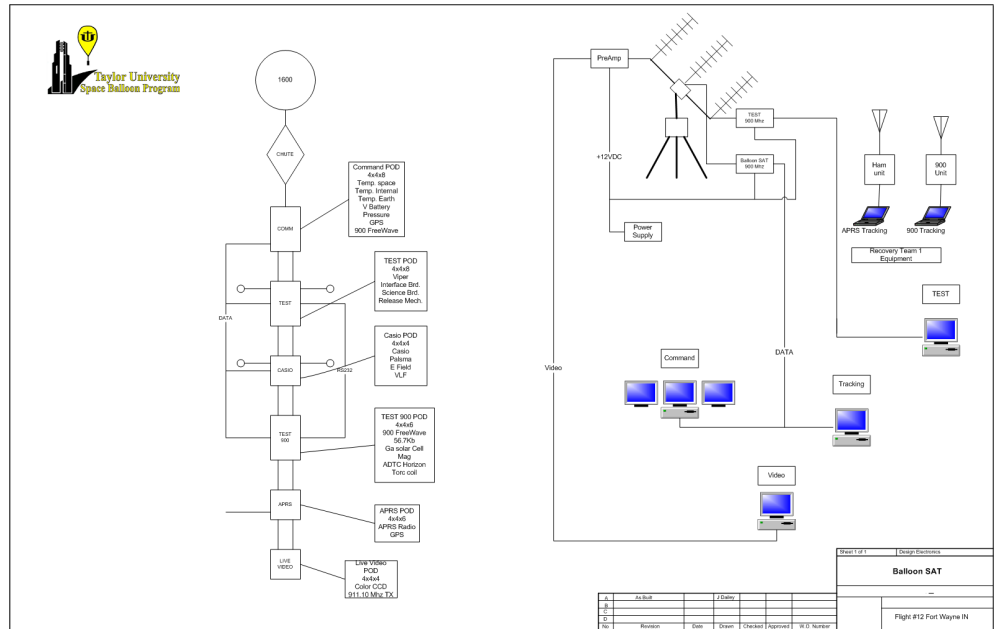


Figure 24. TEST Balloon flight system diagram

XI. SUMMARY

The TEST nanosatellite demonstrates the capability of a high degree of technology while minimizing space, and a high degree of educational value for all involved. Because of the increased modularity and the large number of built in testing capabilities the TEST satellite has the potential to reduce costly satellite construction. Large degrees of freedom given to subsystem teams allows, and encourages, creative designs. Because of the Common Interface Board and the buffered data bus, subsystem teams are able to utilize an ever growing inventory of commercial-off-

the-shelf components, reducing overall satellite costs. The organization structure of compartmentalized subsystems provides for rapid understanding of satellite functions and implementation of designs.

Reduced costs of satellites and standardized modular cubes allows for large multi-probe satellite constellations to be affordable. This has direct application to DOD DMSP and NASA's "Living With a Star" geospace missions. Foundationally the TEST satellite may be a disruptive 3-D technology differing greatly from current spacecraft designs. However, the TEST satellite is a very complementary technology in that it offers a better way for future spacecraft to investigate the universe we live in.

Acknowledgments

The Air Force Office of Space Research (AFOSR) University Nanosatellite Program under contract and the Taylor University Science Research Training Program (SRTP) supported this work. The authors of this paper would like to thank the following for their time and technical involvement in the design and construction of TEST: Dr. Gary Swenson, Dr. Will Holmes and Mr. Adam Bennett and students Matt Hockenheimer, Brad Moser, Andrew Strange, D. Tan, Derek Schmidt, Joel Ahlquist, Noah McCalment, Andrew Ramsay, Matt McGill, Peter Schultz, and Jon Voss. We would also like to thank the many faculty, staff, students and their families who put their time and effort into this project.

References

Periodicals

² Voss, H. D., M. Walt, W. L. Imhof, J. Mobilia, and U. S. Inan, "Satellite observations of lightning-induced electron precipitation", *J. Geophys. Res.*, 103, 1998, pp 11,725-11,744.

³ Swenson, G. R. and C. S. Gardner, Analytical models for the responses of the Mesospheric Na and OH* layers to atmospheric gravity waves, *J. Geophys. Res.*, 103, 1998, pp 6271-6294.

³ Kamalabadi, F., J.M. Forbes, N.M. Makarov, and Yu.I. Portnyagin, "Evidence for nonlinear coupling of planetary waves and tides in the Antarctic mesopause, *Journal of Geophysical Research (Atmospheres)*, Vol. 102, No. D4, 1997, pp 4437-4446.

Proceedings

¹ Heidt, H.; Puig-Suari, J.; Moore, A.; Nakasuka, R.; Twigg, R., "CubeSat: A new Generation of Picosatellite for Education and Industry Low-Cost Space Experimentation," *13th Annual AIAA/USU Conference on Small Satellites* Logan, UT, August 2000.

¹ Puig-Suari, Jordi; Turner, Clark and Twigg, Robert J., CubeSat: The Development and Launch Support Infrastructure for Eighteen Different Satellite Customers on One Launch." *15th Annual AIAA/USU Conference on Small Satellites*, Logan, UT, August 2001.

² Voss, D. L., A. Kirchhoff, D. P. Hagerman, D.C.H Tan, J.J. Zapf, J. Dailey, A. White, H. D. Voss, M. Maple, and Farzad Kamalabadi, "A Highly Modular Scientific Nanosatellite: TEST," *18th Annual AIAA/USU Conference on Small Satellites* Logan, UT, August 2004.

⁶ Voss, H. D., J.B. Reagan, W.L. Imhof, D.O. Murray, D. A. Simpson, D. P. Cauffman and J. C. Bakke, Low-Temperature Characteristics of Solid State Detectors for Energetic X Ray, Ion and Electron Spectrometers, *IEEE Trans. Nucl. Sci.*, NS-29, 1982, pp 173.

Electronics Publications

¹ The CubeSat specification may be downloaded from Stanford's CubeSat home page, <http://ssdl.stanford.edu/cubesat/>.

⁴ These cells do not meet Spectrolab's space specifications and can be purchased at reduced rates on their web site, <http://www.spectrolab.com/stores/>.

⁵ The P-POD is the tube that houses and launches CubeSats into space. For more details, please see Stanford's CubeSat home page, <http://ssdl.stanford.edu/cubesat/>.

⁷ Data on the Spacecraft Control Toolbox (Princeton Satellite Systems) may be found on the PSS web site, www.psatellite.com.

⁸ Information on xPC Target and rapid prototyping for embedded systems may be found on the Mathworks web site, www.mathworks.com.